An Unsaturated Soil Water Flow Problem and Its Numerical Simulation①

Xie Zhenghui (谢正辉), Dai Yongjiu (戴永久) and Zeng Qingcun (曾庆存)

LASG, Institute of Atmospheric Physics, Chinese Academy of Sciences, Beijing 100080

(Received June 8, 1998; revised June 18, 1998)

ABSTRACT

A numerical model for the unsaturated flow equation with moisture content as prognostic variable is established in order to simulate liquid moisture flow in an unsaturated zone with homogeneous soil, and different initial and boundary conditions. For an infiltration or evaporation problem, its numerical solution by using a finite difference method is very sensitive to its upper boundary condition and the related soil parameters, and using a traditional finite element method usually yields oscillatory non-physics profiles. However, we obtain a nonoscillatory solution and evade a non-physics solution for the problem by using the mass-lumped finite element method. This kind of boundary conditions is handled very well. Numerical simulations for certain soils show that the numerical scheme can be used in simulation of liquid moisture flow for infiltration, evaporation, re-distribution and their alternate appearances. It can be also applied to a high-resolution land surface model.

Key words: Unsaturated flow, Finite element, Mass lumping, Numerical simulation

1. Introduction

Unsaturated soil water flow is a flow where water is not full of soil hole, which is an important form of flow in porous media. Prediction of an unsaturated flow is provided with significance in many branches of science and engineering. These include atmospheric science, soil science, agricultural engineering, environment engineering, and groundwater hydrology. Soil water content is an important climate factor, and its seasonal change has an important influence on weather and climate at mid-high latitudes. Land surface parameterization which stresses computation of soil content, is widely concerned (Ye et al., 1991; Dai et al., 1997; Dickinson et al., 1993). Hydraulic processes at surface and subsurface, such as precipitation, evaporation, and evapotranspiration, seepage of surface water, and capillary elevation of deep-level water, absorption in root zone and liquid moisture flow of groundwater, all can be reduced to unsaturated flow problems (Lei et al., 1988; Bear, 1972; Celia et al., 1990; Rathfelder et al., 1994; Xie et al., 1998a). As a matter of fact, in all studies of the unsaturated zone, the fluid motion is assumed to obey the classical Richards equation (Celia et al., 1990). This equation may be written in several forms with either moisture content θ or press head h. Because the equation is nonlinear, its analytical solution is impossible to obtain except for special cases. Therefore numerical approximations are typically used to solve the

①This work was supported by Chinese NSF Project (No. 49735160), the Chinese National Key Project of Fundamental Research "Climate Dynamics and Climate Prediction Theory" (No. 21), and China Postdoctoral Science Foundation.

unsaturated flow equation.

For an infiltration or evaporation problem, its numerical solution by using a finite difference method is very sensitive to its upper boundary condition and the related soil parameters. By using a finite element method, this kind of boundary conditions can be handled very well through reducing calculation of known flux by using variation. Unfortunately, using a traditional finite element method is entirely possible to yield non-physics oscillatory infiltration or evaporation profiles.

In this paper, a numerical model for the unsaturated flow problem with moisture content as prognostic variable is established in order to simulate liquid moisture flow in an unsaturated zone with homogeneous soil, and different initial and boundary conditions. We obtain a nonoscillatory solution and evade a non-physics solution for the problem by using the mass-lumped finite element method. This kind of infiltration and evaporation boundary conditions is handled very well. Numerical simulations for certain soils show that the numerical scheme can be used in simulation of liquid moisture flow for infiltration, evaporation, re-distribution and their alternate appearances. It can be also applied to a high-resolution land surface model.

2. An unsaturated flow problem

2.1 *A vertical infiltration and evaporation problem*

Based on horizontal resolution of a general circulation model (1 to 5 longitude-latitudes resolution), liquid moisture flow in soil along horizontal direction may be ignored. We consider a one-dimensional unsaturated problem. Let z denote the vertical dimension, assumed positive downward, and $\theta(z, t)$ be soil volumetric content at time t and at the distance z from surface. We suppose that the infiltration or evaporation rate at surface dependent of time is given, which is positive for infiltration and negative for evaporation. Moisture content at the bottom of the domain Ω is given dependent of time. Then by Darcy law and continuous principle, we obtain the following unsaturated flow Richards equation:

$$\frac{\partial \theta}{\partial t} - \frac{\partial}{\partial z}\left(D(\theta)\frac{\partial \theta}{\partial z}\right) + \frac{\partial K(\theta)}{\partial z} = S_r \qquad (1)$$

$$\theta(z,0) = \theta_0(z), \quad 0 \leqslant z \leqslant L \qquad (2)$$

$$\theta(L,t) = \beta(t), \quad t > 0 \qquad (3)$$

$$K(\theta) - D(\theta)\frac{\partial \theta}{\partial z} = q(t), \quad \text{if} \quad z = 0, \quad t > 0 \qquad (4)$$

where $\theta[L^3 / L^3]$ is soil moisture, $D(\theta)$ the soil water diffusivity, $K(\theta)[LT^{-1}]$ the unsaturated hydraulic conductivity, $-S_r[L^3 T^{-1} L^{-3}]$ absorption rate of root zone, and $q(t)$ the infiltration or evaporation rate at upper boundary $z = 0$, see Lei et al. (1988), Bear (1972), Celia et al. (1990), Haverkamp et al. (1977), Rathfelder et al. (1994). The presumed conditions (2)-(4) are initial condition, lower boundary condition, upper boundary condition, respectively. The upper boundary condition has the following cases.

- When $q(t) > 0$, (4) is equivalent to the case in which the known surface flux does not exceed the infiltration intensity, and does not generate runoff.

• When the surface flux exceeds the infiltration intensity, and runoff generates, the boundary condition (4) is substituted for

$$\begin{cases} K(\theta) - K(\theta)\dfrac{\partial \theta}{\partial z} = q(t) \text{ when } z = 0 \text{ and } t_a > t > 0 , \\ \theta(0,t) = \theta_s \text{ when } t \geqslant t_a , \end{cases} \tag{5}$$

here t_a is the beginning time when it exceeds the infiltration strength, and is taken as the beginning time of $\theta(0, t) = \theta_s$ since $\theta \leqslant \theta_s$ (θ_s –saturated moisture content).

• When $q(t) \leqslant 0$, the upper boundary condition (4) is equivalent to the case in which soil at surface is evaporated at evaporation rate $q(t)$.

• When soil at surface is evaporated at evaporation rate $q(t)$, and moisture content at surface reaches the air–dried rate after time t_a, the boundary condition (4) is substituted for

$$\begin{cases} K(\theta) - D(\theta)\dfrac{\partial \theta}{\partial z} = q(t) \text{ when } z = 0 \text{ and } t_a > t > 0 , \\ \theta(0,t) = \theta_d \text{ when } z = 0 \text{ and } t \geqslant t_a , \end{cases} \tag{6}$$

here t_a is the beginning time when that reaches the air–dried rate, and is taken as the beginning time of $\theta = \theta_d$ since $\theta \geqslant \theta_d$.

• When soil at surface keeps saturated, and is evaporated after time t_a, the boundary condition (4) is substituted for

$$\begin{cases} \theta(0,t) = \theta_s \quad \text{when} \quad z = 0 \quad \text{and} \quad t_a > t > 0 , \\ K(\theta) - D(\theta)\dfrac{\partial \theta}{\partial z} = q(t) \quad \text{when} \quad z = 0 \quad \text{and} \quad t \geqslant t_a , \end{cases} \tag{7}$$

here t_a is the beginning time when $q(t) < 0$.

• When soil at surface keeps air–dried rate θ_d, and infiltrates after time t_a, the boundary condition (4) is substituted for

$$\begin{cases} \theta(0,t) = \theta_d \quad \text{when} \quad z = 0 \quad \text{and} \quad t_a > t > 0 , \\ K(\theta) - D(\theta)\dfrac{\partial \theta}{\partial z} = q(t) \quad \text{when} \quad z = 0 \quad \text{and} \quad t > t_a , \end{cases} \tag{8}$$

here t_a is the beginning time when $q(t) > 0$.

In most of land–surface models, the following fitting–relations are taken (c.f. Campbell, 1974):

$$\begin{cases} K(\theta) = K_s \left(\dfrac{\theta}{\theta_s}\right)^{2b+3} , \\ \Psi(\theta) = \Psi_s \left(\dfrac{\theta}{\theta_s}\right)^{-b} , \\ D(\theta) = -\dfrac{bK_s\Psi_s}{\theta_s} \left(\dfrac{\theta}{\theta_s}\right)^{b+2} . \end{cases} \tag{9}$$

Here, $K_s > 0$, $\psi_s < 0$, $0 < \theta_s < 1$.

2.2 *Extremum principle*

About the problems (1)–(4), with the expression in (9), we can prove the following properties, which can be refered to Xie et al (1998c).

Property 1. If it evaporates at upper boundary $z = 0$, i.e. $q(t) \leqslant 0$, the source–sink $S_r = 0$, and the initial condition $\theta_0(z)$ reaches its minimum at upper boundary $z = 0$ and its maximum at lower boundary $z = L$, $\beta(t) = \theta_0(L)$ is a constant independent of time t, then for $\forall t_0$, $\theta(z, t_0)$ in problems (1)–(4) reaches its minimum at $z = 0$ and its maximum at $z = L$.

Property 2. If it infiltrates at upper boundary $z = 0$ with infiltration rate $q(t) \geqslant K(\theta_s)$ at $z=0$, the source–sink $S_r = 0$, and the initial condition $\theta_0(z)$ reaches its maximum at upper boundary $z=0$ and its minimum at lower boundary $z = L$, $\beta(t) = \theta_0(L)$ is a constant independent of time t, then for $\forall t_0 \theta(z, t_0)$ in problems (1)–(4) reaches its maximum at $z = 0$ and its minimum at $z = L$.

These two properties show that the mathematical models (1)–(4) satisfy its extremum principle, which coincides with physical properties.

3. A numerical model using a finite element approximation

As an example we consider the problems (1–4) and explain numerical simulation processes of the model.

3.1 *The second kind of upper boundary condition*

Let $H_E^1(\Omega) = \{v \in H^1(\Omega), v(L) = 0\}$, here $H^1(\Omega)$ is a Sobolev space, up to the first derivatives of which are square integrable (Adams et al., 1975) on Ω. Set $\theta(z, t) = \bar{\theta}(z,t) + \beta(t)$, and homogenize the lower boundary condition. We have

$$\begin{cases} \dfrac{\partial \bar{\theta}}{\partial t} = \dfrac{\partial}{\partial z}\left(D(\theta)\dfrac{\partial \theta}{\partial z}\right) - \dfrac{\partial K(\theta)}{\partial z} - \dfrac{d\beta}{dt} + S_r, \quad (z,t) \in \Omega \times (0,T), \\ \bar{\theta}(z,0) = \theta_0(z) - \beta(0), \quad 0 \leqslant z \leqslant L, \\ \bar{\theta}(L,t) = 0, \quad t > 0, \\ K(\theta) - D(\theta)\dfrac{\partial \theta}{\partial z} = q(t), \quad t \in (0,T), \quad \text{at} \quad z = 0, \\ \bar{\theta}(z,t) = \theta(z,t) - \beta(t). \end{cases} \tag{10}$$

The equivalent variational formulation of the considered problem is as follows:

$$\begin{cases} \text{to find} \quad \theta(z,t) \in H_E^1(\Omega), \quad \forall t \in (0,T), \quad \text{such that} \quad \forall \varphi \in H_E^1(\Omega), \\ \left(\dfrac{\partial \bar{\theta}}{\partial t}, \varphi\right) + \left(D(\theta)\dfrac{\partial \bar{\theta}}{\partial z}, \dfrac{\partial \varphi}{\partial z}\right) = -q\,\varphi|_0^L + \displaystyle\int_0^L K(\theta)\dfrac{\partial \varphi}{\partial z}dz + (S_r, \varphi) - (\beta'(t), \varphi), \end{cases} \tag{11}$$

where and from now on $(\cdot, \cdot)$ denotes the L^2–inner product on Ω (see Adams, 1975). Since variation of $\beta(t)$ is small relatively, so we omit the term $\left(\frac{d\beta}{dt}, \varphi\right)$ in the computation.

3.1.1 *Semi–discrete finite element approximation*

We first introduce finite element approximation in space direction. Divide the domain $\Omega = (0,L)$ such that $0 = z_0 < z_1 < z_2 < \cdots < z_{n+1} = L$, where z_0 and z_{n+1} are the boundary points of domain Ω. Let $e_i = (z_i, z_{i+1})(i = 0, \cdots, n)$ be $n + 1$ elements. Define a finite element space $V_h \subset H_E^1(\Omega)$ such that $V_h = \{v_h$ is continuous in [0,1], $v_h|e_i$ is linear polynomial for $0 \leqslant i \leqslant n$ and $v_h(L) = 0\}$.

Let $\{\varphi_i\} \subset V_h$ be the finite element basic functions (Ciarlet, 1978), $\varphi_i(z_j) = \delta_{ij}(i,j= 0, \cdots, n + 1)$. Since $\bar{\theta} \in V_h$, $\theta(z, t) = \sum_{i=0}^{n} X_i(t)\varphi_i(z) + \beta(t)$. Therefore, the matrix formulation of semi-discrete finite element approximation of the problem (10) or (11) may be written as follows:

$$\begin{cases} [A]\{X\}+[B]\left\{\dfrac{dX}{dt}\right\}=\{F\} \ , \\ \{X(0)\}=(\theta_0(z_0)-\beta(0),\cdots,\theta_0(z_0)-\beta(0))^T \ , \end{cases} \tag{12}$$

where

$$\begin{cases} [A]=[A_{ij}], \quad A_{ij}=\displaystyle\int_0^L D(\theta)\frac{d\varphi_i}{dz}\frac{d\varphi_j}{dz}dz \ , \\ [B]=[B_{ij}], \quad B^{ij}=\displaystyle\int_0^L \varphi_i\varphi_j dz \ , \\ \{F\}=[F_i], \quad F_i=-q\ \varphi_i\big|_0^L+(S_r,\varphi_i)+\displaystyle\int_0^L K(\theta)\frac{d\varphi_i}{dz}dz-(\beta'(t),\varphi) \ , \\ \{X\}=(X_0(t),\cdots,X_n(t))^T \ , \\ \left\{\dfrac{dX}{dt}\right\}=\left(\dfrac{dX_0}{dt},\cdots,\dfrac{dX_n}{dt}\right)^T \ , \quad i,j=0,\cdots,n \ . \end{cases} \tag{13}$$

Equation (12) defines a set of ordinary differential equations with non-linear coefficients. To get a numerical solution of the problem, discretization for time variable should be introduced.

3.1.2 *A full discrete scheme*

A finite difference scheme may be introduced to approximate the time derivatives in the matrix equation, and then the Galerkin finite element-finite difference scheme of problem (11) is obtained. Define for that purpose the following approximations:

$$\begin{cases} \left\{\dfrac{dX}{dt}\right\}\approx\dfrac{\{X\}^{t+\Delta t}-\{X\}^t}{\Delta t} \ , \\ \{X\}^{t+\Delta t/2}\approx\omega\{X\}^{t+\Delta t}+(1-\omega)\{X\}^t \ , \end{cases} \tag{14}$$

where Δt is the time step and ω a temporal weighting coefficient. By defining matrix equation (12) at the half-time level $(t+\Delta t/2)$, and introducing approximations in (14), the following algebraic equation system results:

$$[A]^{t+\Delta t/2}(\omega\{X\}^{t+\Delta t}+(1-\omega)\{X\}^t)+[B]^{t+\Delta t/2}\frac{\{X\}^{t+\Delta t}-\{X\}^t}{\Delta t}=\{F\}^{t+\Delta t/2} \ .$$

And then

$$[P]^{t+\Delta t/2}\{X\}^{t+\Delta t}=[Q]^{t+\Delta t/2}\{X\}^t+\{F\}^{t+\Delta t/2} \ , \tag{15}$$

where

$$\begin{cases} [P]=\omega[A]+\dfrac{1}{\Delta t}[B] \ , \\ [Q]=(\omega-1)[A]+\dfrac{1}{\Delta t}[B] \ . \end{cases} \tag{16}$$

When $\omega=1$ an implicit in time finite difference scheme results, even through the various coefficients are evaluated at the half-time level. When $\omega=1/2$, on the other hand, a time-centred, Crank-Nicolson type algorithm is obtained. To be able to solve equation (15), one needs estimates of the coefficient K and D and then coefficient matrix $[A]$, $[B]$, $[F]$ in equation (16) and $[P]$, $[Q]$ in equation (15) at the half-time level. Since the mass-lumped finite element method is used in computation, and all elements in each row are summed up into the main-diagonal element, oscillatory non-physics profiles are evaded. Because elements of these matrix depend on the soil content, it is necessary to have an estimate of the moisture content distribution θ at the half-time level. For each new time step this distribution is obtained through linear extrapolation from the old distributions as follows:

$$\theta^{t+\Delta t/2}=\theta^{t}+\frac{\Delta t_n}{2\Delta t_0}(\theta^{t}-\theta^{t-\Delta t}) , \qquad (17)$$

where Δt_n and Δt_0 are old and new time increments, respectively. Expression (14) is a kind of approximations, which may be improved by means of pre-estimate and correct iteration processes. During each iteration the most recent distribution of $\theta_0^{t+\Delta t}$ obtained by solving equation (15), is used to obtain a new estimate for the half-time level: $\theta^{t+\Delta t/2}=\frac{1}{2}(\theta_0^{t+\Delta t}+\theta^{t})$. By using $\theta^{t-\Delta t/2}$, a new moisture content $\theta_n^{t+\Delta t}$ may be obtained by solving equation (15). The iterative process continues until a satisfactory degree of convergence is obtained. The criterion of convergence, in its most general form, is given by: $|\theta_n^{t+\Delta t}-\theta_0^{t+\Delta t}|\leqslant\mu_1+\mu_2|\theta_n^{t+\Delta t}|$, where k represents the iteration number, and μ_1, μ_2 are the selected absolute and relative error criteria.

To compute moisture content distribution at a new time level, the first step is to estimate $\theta^{t+\Delta t/2}$ soil content distribution at the half-time step. If the time level is not the first one, it can be pre-estimated through linear extrapolation according to (17). However, if the time level is the first one, it cannot do like this since only initial distribution is known. In this case, the initial distribution may be taken as the pre-estimated distribution at the first half time level.

3.1.3 *Discrete extremum principle*

Since the physical problem and the mathematical models (1)-(4) satisfy the so-called extremum properties (c.f. property 1 and property 2 in Section 2.2), it requires the discrete problems (12) and (15) to satisfy the properties. We have the following theorem.

Theorem 1. By summing up all elements in each row of matrix B into the main-diagonal element, we get a matrix and still call it matrix B. When the time step is small suitably, then the matrixes P and Q in (15) satisfy that:

(i) P is positive definite matrix, and its non-diagonal elements are non-positive;

(ii) matrix $P^{-1}Q$ is positive matrix, i.e. its elements are larger than or equal to zero;

(iii) each row of matrix $P^{-1}Q$ is less or equal to 1.

When $\omega=1$ in (14) or (16), the conclusion is true for arbitrary time step.

Hence it shows that the discrete scheme by using the mass-lumped finite element method satisfies extremum principle.

However, (i)-(iii) in the theorem do not hold in general for the matrixes P,Q in (15) by using a finite element method without the mass lumping. Theorem 1 in this case does not satisfy the extremum principle in general, and it usually generates a non-physics solution. We omit the proof here.

3.2 *The first boundary condition*

Consider problem (1) with initial condition (2), low boundary condition (3) and the upper boundary condition $\theta(0,t)=\alpha(t)$, Let $H_0^1(\Omega)=\{v\in H^1(\Omega), v(0)=v(L)=0\}$. Set

$$\theta(z,t)=\bar{\theta}(z,t)+\frac{\beta(t)-\alpha(t)}{L}z+\alpha(t)\ ,$$

and then homogenize the lower boundary condition. We have

$$\begin{cases}\dfrac{\partial\bar{\theta}}{\partial t}=\dfrac{\partial}{\partial z}\left(D(\theta)\dfrac{\partial\theta}{\partial z}\right)-\dfrac{\partial K(\theta)}{\partial z}-\dfrac{\beta'(t)-\alpha'(t)}{L}z-\alpha'(t)+S_r,\ (z,t)\in\Omega\times(0,T)\ ,\\ \bar{\theta}(z,0)=\theta_0(z)+\dfrac{\beta(0)-\alpha(0)}{L}z+\alpha(0),\ 0\leqslant z\leqslant L\ ,\\ \bar{\theta}(0,t)=\bar{\theta}(L,t)=0,\quad t>0\ ,\\ K(\theta)-D(\theta)\dfrac{\partial\theta}{\partial z}=q(t),\quad t\in(0,T),\quad \text{at}\quad z=0\ ,\\ \bar{\theta}(z,t)=\theta(z,t)-\dfrac{\beta(t)-\alpha(t)}{L}z-\alpha(t)\ .\end{cases}\tag{18}$$

Then the related equivalent variational formulation of the considered problem (18) is as follows:

$$\begin{cases}\text{to find}\quad \theta(z,t)\in H_0^1(\Omega),\ \forall t\in(0,T),\quad \text{such that}\ \forall\varphi\in H_0^1(\Omega)\ ,\\ \left(\dfrac{\partial\bar{\theta}}{\partial t},\varphi\right)+\left(D(\theta)\dfrac{\partial\bar{\theta}}{\partial z},\dfrac{\partial\varphi}{\partial z}\right)=\displaystyle\int_0^L K(\theta)\frac{\partial\varphi}{\partial z}dz+(S_r,\varphi)-\left(\alpha'(t)+\frac{\beta'-\alpha'(t)}{L}z,\varphi\right)\ .\end{cases}\tag{19}$$

Since viriation of $\alpha(t)$ and $\beta(t)$ is small relatively, so we assume $\alpha'(t),\beta'(t)\approx 0$ in the computation.

As in Section 3.1.1 we introduce finite element approximation in space direction. Define a finite element space $V'_h\subset H_0^1(\Omega)$ such that $V'_h=\{v_h$ is continuous in $[0,1]$, $v_h|e_i$ is linear polynomial for $0\leqslant i\leqslant n$ and $v_h(0)=v_h(L)=0\}$.

Let $\{\varphi_i\}\subset V'_h$ be the finite element basic functions (Ciarlet, 1978), $\varphi_i(z_j)=\delta_{ij}(i,j=1,\cdots,n)$. Since $\bar{\theta}\in V'_h$, we have

$$\theta(z,t)=\sum_{i=1}^{n}X_i(t)\varphi_i(z)+\frac{\beta(t)-\alpha(t)}{L}z+\alpha(t)\ .$$

Therefore, the matrix formulation of a semi-discrete finite element approximation for the problem (18) or (19) may be written as follows:

$$\begin{cases}[A]\{X\}+[B]\left\{\dfrac{dX}{dt}\right\}=\{F\}\ ,\\ \{X(0)\}=\left(\theta_0(z_0)-\dfrac{\beta(0)-\alpha(0)}{L}z_0,\cdots,\theta_0(z_n)-\dfrac{\beta(0)-\alpha(0)}{L}z_n\right)^T\ ,\end{cases}\tag{20}$$

where

$$\begin{cases} [A]=[A_{ij}], \quad A_{ij}=\int_0^L D(\theta)\frac{d\varphi_i}{dz}\frac{d\varphi_j}{dz}dz \ , \\ [B]=[B_{ij}], \quad B_{ij}=\int_0^L \varphi_i\varphi_j dz \ , \\ \{F\}=[F_i], \quad F_i=(S_r,\varphi_i)+\int_0^L(\alpha'+\frac{\beta'-\alpha'}{L}z)\varphi dz+\int_0^L K(\theta)\frac{d\varphi_i}{dz}dz \ , \\ \{X\}=(X_0(t),\cdots,X_n(t))^T \ , \\ \left\{\frac{dX}{dt}\right\}=\left(\frac{dX_0}{dt},\cdots,\frac{dX_n}{dt}\right), \quad i,j=1,\cdots,n \ . \end{cases} \tag{21}$$

Equation (20) defines a set of ordinary differential equations with non-linear coefficients. The finite difference scheme (14) can be introduced to approximate the time derivatives in the matrix equation (20), and then the Galerkin finite element-finite differential scheme of the problem (18) or (19) is obtained as (15), which can be resolved similarly as in Section 3.1.3. We can get similar results for the problem with the first kind of boundary condition.

3.3 *Alternative cases*

In Section 2, we can see that in the alternative cases, how to determine t_a in (5), (6), (7) and (8), is very important, which is the turning point time of the upper boundary condition. At each time t, we determine the upper boundary condition in the next step $t+\Delta t$ according to the following principle.

(i) If the upper boundary condition is (5), $\theta(0,t)=\theta_s$ and $q(t+\Delta t)>0$, then the first kind of boundary condition $\theta(0,t)=\theta_s$ is used in next step, $t_a=t+\Delta t$.

(ii) If the upper boundary condition is (6), $\theta(0,t)\leqslant\theta_d$ and $q(t+\Delta t)<0$, then the first kind of boundary condition $\theta(0,t)=\theta_d$ is used in next step, $t_a=t+\Delta t$.

(iii) If the upper boundary condition is (7), $\theta(0,t)=\theta_s$ and $q(t+\Delta t)\leqslant 0$, then the second kind of boundary condition $K(\theta)-D(\theta)\frac{\partial\theta}{\partial z}=q(t)$ is used in next step, $t_a=t+\Delta t$.

(iv) If the upper boundary condition is (8), $\theta(0,t)=\theta_d$ and $q(t+\Delta t)>0$, then the second kind of boundary condition $K(\theta)-D(\theta)\frac{\partial\theta}{\partial z}=q(t)$ is used in next step, $t_a=t+\Delta t$.

4. Numerical simulation

The soil parameters K_s, Ψ_s, θ_s and B for eleven soils were assigned in Clapp et al. (1978), Cosby et al. (1984), Henderson-Selles et al. (1986), Wilson et al. (1985), Dickinson et al. (1993).We give the parameters for the twelve soils as the following table according to Dickinson et al. (1993).

4.1 *The case for the eighth soil*

The soil parameters for the eighth soil in (9) are as follows: $\theta_s=0.54$, $\psi_s=-200$ (mm), $K_s=3.2\times10^{-3}$ (mm / s), $B=7.6$, $\theta_d/\theta_s=0.419$, $L=200$ cm. In Section 4, we divide the domain $\Omega=(0,200)$ into two hundred elements.

Table 1. Soil parameters for 12 soils

soil type\parameters	θ_s	$-\psi_s$ (mm)	K_s (mm / s)	B	θ_d / θ_s
1	0.33	30	0.2	3.5	0.088
2	0.36	30	0.08	4.0	0.119
3	0.39	30	0.0032	4.5	0.151
4	0.42	200	0.013	5.0	0.266
5	0.45	200	8.9e-3	5.5	0.300
6	0.48	200	6.3e-3	6.0	0.332
7	0.51	200	4.5e-3	6.8	0.378
8	0.54	200	3.2e-3	7.6	0.419
9	0.57	200	2.2e-3	8.4	0.455
10	0.60	200	1.6e-3	9.2	0.487
11	0.63	200	1.1e-3	10.0	0.516
12	0.66	200	0.8e-3	10.8	0.542

4.1.1 *Stable infiltration and evaporation*

We assume that a constant moisture content 0.226 was maintained at the lower end of the column and a constant infiltration flux (1.0×10^{-1} cm / hour) was imposed at the soil surface ($z = 0$) during 450 hours since the beginning of infiltration. Assumed that after 450 hours, evaporation began at the evaporation rate 1.0×10^{-2} cm / hour. The initial and boundary conditions for infiltration and evaporation of water in the soil were

$$\begin{cases} \theta(z,0) = 0.226, \quad z \in [0,200] \ , \\ q(t) = \begin{cases} 0.1\text{cm / hour, when} \quad 0 < t < 450 \text{ hours} \ , \\ q = -0.01 \text{ cm / hour, when } 450 \leqslant t \leqslant 1000 \text{ hours} \ , \end{cases} \\ \theta(200,t) = 0.226 \ . \end{cases} \tag{22}$$

The time step $\Delta t = 2.5$ hour. Those dates were included into the program. The obtained soil moisture profiles at each 25 hours from 1 to 450 hours, are presented in Fig. 1. Here the abscissa denotes moisture content, the ordinate denotes depth (cm) from surface, and each curve denotes a soil moisture profile at certain time. There are no oscillatory non-physics profiles for the monotone infiltration problem. Fig. 2 presents infiltration and evaporation profiles at each 125 hours period.

It may be seen from Fig. 1 and Fig. 2 that moisture content at surface increased from 0.226 to saturated moisture content rapidly during 125 hours since infiltration occurring. After that time it changed a little and gradually closed to the saturated soil moisture. When $t \geqslant 450$ hours, soil at surface was evaporated at intensity 1.0×10^{-2} cm / hour, i. e. $q = -0.01$ cm / hour, and moisture content at surface decreased rapidly. This coincides with the case in practice.

4.1.2 *Wave infiltration and evaporation*

We assume that a constant moisture content was maintained at the lower end of the column and a constant flux (1.0×10^{-1} cm / hour) was imposed at soil surface ($z = 0$) during 250 hours since the begining of infiltration. Assume that after 250 hours, wave infiltration and evaporation began at rate $q(t) = \sin\frac{\pi t}{30}$ cm / hour. The initial and boundary conditions for infiltration of water in the soil were

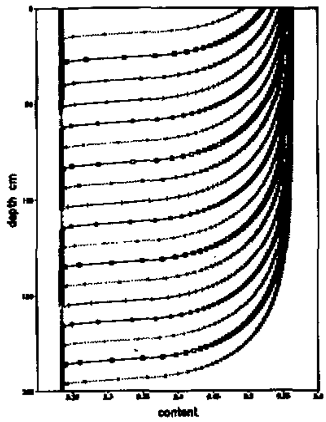

Fig. 1. Soil moisture profiles at each 25 hours.

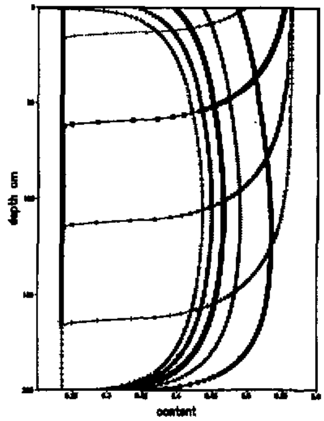

Fig. 2. Infiltration and evaporation.

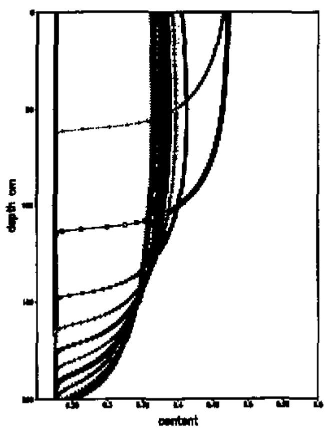

Fig. 3. Wave infiltration and evaporation.

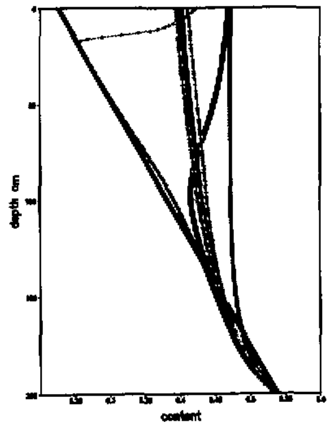

Fig. 4. Wave infiltration and evaporation.

$$\begin{cases} \theta(z,0)=0.226, \quad z\in[0,200] \ , \\ q(t)=\begin{cases} 0.1 \text{ cm / hour, when } \ 0<t<250 \text{ hour} \\ q=\sin\dfrac{\pi t}{30} \text{ cm / hour, when } \ 250\leqslant t\leqslant 1440 \text{ hour} \end{cases} \\ \theta(200,t)=0.226 \ . \end{cases} \tag{23}$$

The time step $\Delta t = 2.5$ hour. Those dates were included into the program. The obtained soil moisture profiles at initial time and at each 125 hours period afterwards are presented in Fig. 3. It may be seen from Fig. 3 that, when evaporation began, soil moisture at surface decreased. Because of the gravity flow, the front of soil moisture approaching to the lower boundary moved forward. After 250 hours since the beginning of wave infiltration and evaporation, moisture content decreased a little. Fig. 4 gives the case when the initial condition in

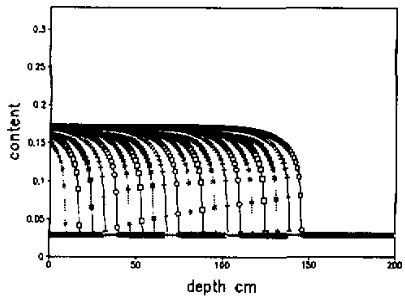

Fig. 5. Soilmoisture profilesateach 10 hours for soil 1.

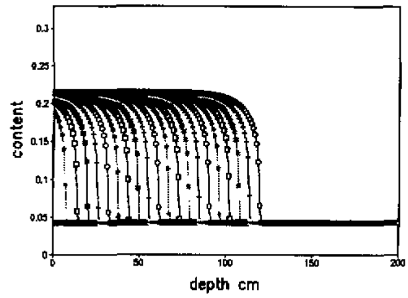

Fig. 6. As in Fig. 5 but for soil 2.

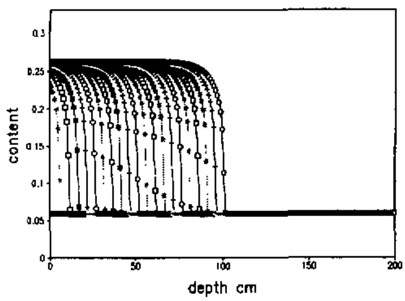

Fig. 7. As in Fig. 5 but for soil 3.

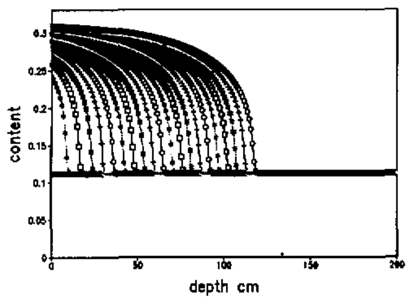

Fig. 8. As in Fig. 5 but for soil 4.

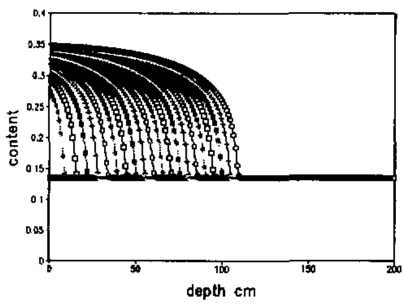

Fig. 9. As in Fig. 5 but for soil 5.

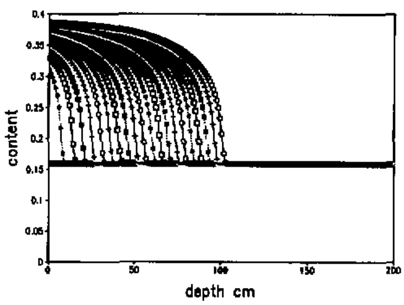

Fig. 10. As in Fig. 5 but for soil 6.

(23) was substituted by $\theta(z, 0) = 0.226 + 0.314 / 200z$, $z \in [0,200]$.

This shows that the numerical model can simulate infiltration, evaporation, and their alternate appearances, and that the results coincided with practice cases.

4.2 *The cases for the twelve soils*

Set $L = 200$ cm. For all the twelve soils, we assume that a constant moisture content θ_d

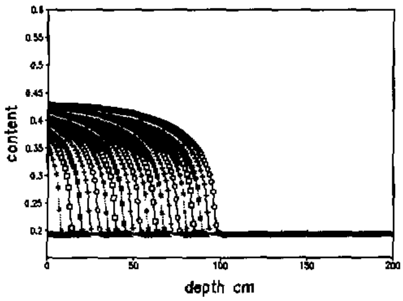

Fig. 11. As in Fig. 5 but for soil 7.

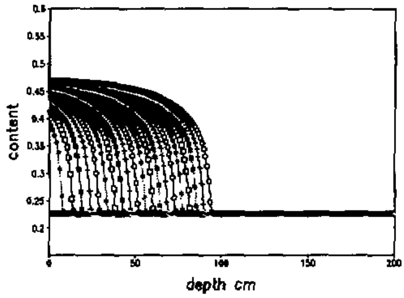

Fig. 12. As in Fig. 5 but for soil 8.

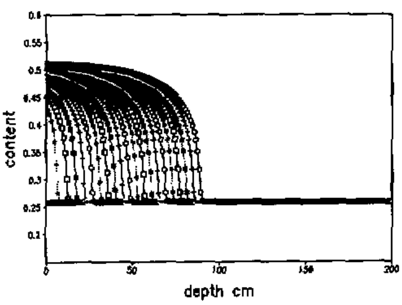

Fig. 13. As in Fig. 5 but for soil 9.

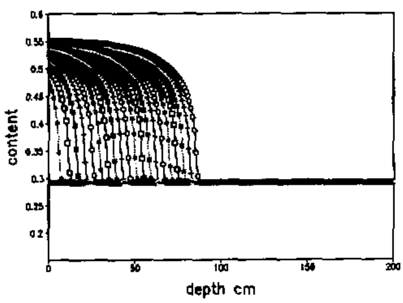

Fig. 14. As in Fig. 5 but for soil 10.

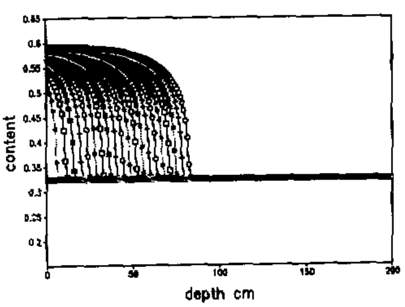

Fig. 15. As in Fig. 5 but for soil 11.

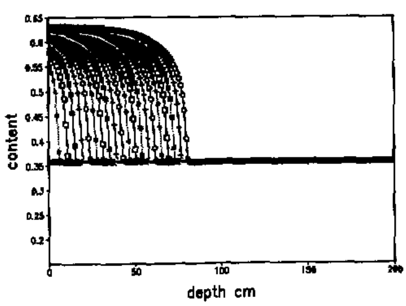

Fig. 16. As in Fig. 5 but for soil 12.

was maintained at the lower end of the column and a constant infiltration flux (1.0×10^{-1} cm / hour) was imposed at the soil surface ($z = 0$) during 250 hours since the beginning of infiltration. Assumed that after 450 hours, evaporation began at the evaporation rate 1.0×10^{-2} cm / hour. The initial and boundary conditions for infiltration and evaporation of water in the soil were

$$\begin{cases} \theta(z,0) = \theta_d, \ z \in [0,200] \ , \\ q(t) = 0.1 \ \text{cm / hour, when} \ 0 \leqslant t \leqslant 250 \ \text{hours} \ , \\ \theta(200,t) = \theta_d \ . \end{cases} \tag{24}$$

The time step $\Delta t = 1$ hour. Those dates were included into the program. The obtained soil moisture profiles at each 10 hours from 1 to 200 hours, are presented in Fig. 5–Fig. 16.

5. Conclusions and discussions

A numerical model for the θ–form unsaturated flow problem by using the mass–lumped finite element method is established in order to simulate liquid moisture flow in unsaturated zone with homogeneous soil, and under different initial and boundary conditions. Infiltration and evaporation boundary conditions are handled through reducing to calculation of known boundary flux by using variation. Numerical results show that the model evades oscillatory non–physics solutions by using the mass–lumped finite element method, and can be used in simulation of liquid moisture flow for infiltration, evaporation, evapotranspiration, re–distribution, and their alternate appearances. It can be also applied to land surface models.

We would like to thank Professor Wang Bin for valuable discussions.

REFERENCES

Adams, R. A., 1975: *Sobolev Spaces*. New York, Academic Press, 26–74.

Bear, J., 1972: *Dynamics of Fluids in Porous Media*. American Elsevier Publishing Company Inc.

Campbell G. S., 1974: A simple method for determining unsaturated conductivity from moisture retention data. *Soil Science*, **117**, 311–314.

Celia, M. A., E. T. Bouloutas, and R. L. Zarba, 1990: A general mass conservation numerical solution for the unsaturated flow equation. *Water Resour. Res.*, **26(7)**, 1483–1496.

Ciarlet, P. C., 1978: *The finite element methods for elliptic problems*. North–Holland.

Clapp, R. B., and G. M. Honberger, 1978: Empirical equations for soil hydraulic properties. *Water Resour. Res.*, **14**, 601–604.

Cosby, B. J., G. M. Hornberger, R. B. Clapp, and T. R. Ginn, 1984: A statistical exploration of the relationships of soil moisture characteristics to the physical properties of soil. *Water Resour. Res.*, **20**, 682–690.

Dai Yongjiu, Zeng Qingcun, 1997: A land surface model (IAP94) for Climate Studies, Part I: formulation and validation in off–line experiments. *Advances in Atmospheric Sciences*, **14(4)**, 433–460.

Dickison, R. E., A. Henderson–Sellers, and P. J. Kennedy, 1993: *Biosphere Atmosphere Transfer Scheme (BATS) version 1e as coupled to the NCAR Community Climate Model*. NCAR Technical Note, NCAR / TN 387+STR.

Haverkamp R., M. Vauclin, and J. Touma et al., 1977: A comparison of numerical simulation models for one–dimensional infiltration. *Soil Sci. Soc. Amer. J.*, **41**, 285–294.

Henderson–Sellers A., M. F. Wilson, G. Thomas, and R. E. Dickison, 1986: *Current Global Land–Surface Data sets for use in Climate–Related Studies*. NCAR Technical Note, NCAR / TN–272+STR.

Rathfelder K., and M. A. Linda, 1994: Mass conservative numerical solutions of the head–based Richards equation. *Water Resour. Res.*, **30(9)**, 2579–2586.

Lei Zhidong, Yang Shixiu, Xie Songcuan, 1988: *Soil Hydrology*, Beijing, Tsinghua University Press (in Chinese).

McCumber, M. C., and R. A. Pielke, 1981: Simulation of the Effects of Surface Fluxes of Heat and Moisture in a Mesoscale Numerical Model, Part I: Soil Layer. *J. Geophys. Res.*, **86**, 9929–9938.

Wilson, M. F., and A. Henderson–Sellers, 1985: A global archive of land cover and soils data for general circulation climate model. *J. Climatology*, **5**, 119–143.

Xie Zhenghui, Zeng Quncun, Dai Yongjiu and Wang Bin, 1998a: Numerical simulation of the unsaturated equation. *Science in China*, **28(2)**, 175–180.

Xie Zhenghui, Zeng Quncun, Dai Yongjiu and Wang Bin, 1998b: An application of the mass-lumped finite element method to the unsaturated soil water flow problem. *Studies in Climate and Environment* **3(1)**, 73–81 (in Chinese).

Xie Zhenghui, Jian Huaiyu, Zeng Quncun and Dai Yongjiu, 1998c: *An extreme principle for the unsaturated soil water flow problem*. to be published (in Chinese).

Xue Y. K., P. J. Sellers, J. L. Kinter, and J. Shukla, 1991: A simplified biosphere model for global climate studies. *J. Climate*, **4**, 345–364.

Ye Duzheng, Zeng Qingcun and Guo Yufu, 1991: *Model Climate Studies*. Beijing, China Meteorological Press, 353 pp (in Chinese).